TRANSACTION ON CONTROL AND MECHANICAL SYSTEMS, VOL. 1, NO. 7, PP. 290-299, NOV., 2012.

Transaction Series on Engineering Sciences and Technologies

Numerical Assessments of Impingement Flow over Flat Surface due to Single and Twin Circular Long Water Jets

M. M. Seraj[1,✉], E. Mahdi[2], and M.S. Gadala[3]

Abstract: **Hydrodynamics of impingement flow is a key partner of heat transfer analysis of run-out table (ROT) steel cooling. Velocity and pressure profiles before and after impingement of long circular free-surface industrial water jets (Re = 16,669-50,068) was numerically studied and also wetting front propagation and size of impingement zone were computed. The turbulent models represented impingement water flows over surface better in good agreement with the experimental data at the ROT facility. Higher velocity gradient was obtained for long turbulent jets indicating enhanced heat transfer at impingement zone. The effect of local pressure on saturation temperature changes predication of boiling heat transfer correlations up to 9% which is noticeable for ROT cooling. Impingement zone was found smaller respect to the estimation used in ROT modeling obtained from short jets experiments. For twin jets, simulation show calm interaction of low flow rate water jets with no splashing in accordance with the experiment. Water film thickness in interaction zone is elevated toward jet-jet axis.**

Keywords: Long Jet, Hydrodynamics, Run-Out Table, Jet Interaction, Cooling.

1. INTRODUCTION

Liquid jet impingement with distinguished ability in cooling has been used widely in different industries such as electronic packages [1] and metal making processes [2-3]. In steel making industry, arrays of water jets cool red hot steel strip to a specified temperature in run-out table (ROT) stage before coiling. The control of cooling in ROT is crucial in order to obtain desirable mechanical properties (e.g. toughness, strength) and metallurgical properties (e.g. microstructure, hardness) according to customers demand. New advanced high strength steels are increasingly developed at reduced coiling temperature of steel strip and, in turn, sophisticated cooling systems with more accurate thermal prediction have to be employed at ROT stage. However, ROT cooling is a highly complicated transient heat transfer process and full scale modelling is a very difficult task. In fact, ROT modeling significantly relies on practical experiences and experimental data of boiling heat transfer researches. Reported studies on boiling jet impingement were usually small scale experiments of single water jet impinging on stationary test surface and, in which, investigate the effect of relevant parameters and conditions such as boiling regimes, jet velocity, jet diameter, nozzle-to-plate distance, water temperature, surface initial temperature, etc (see [4] as an extensive review).

At single jet impingement, water flow due to circular jet is spreading radially in impingement zone and is thinning in parallel (wall) zone where radial flow motion is slowed down and eventually may terminate with a hydraulic jump. Various boiling/nonboiling regimes and heat transfer mechanisms occur over hot surface depend on both hydrodynamics of impingement coolant flow and thermal characteristics in wetted and nonwetted areas. For example, local heat transfer coefficient between impingement flow and substrate is found to be linked to flow parameters [5] and maximum heat flux is usually detected at vicinity of wetting front where sudden changes in surface temperature and heat flux is detected [6]. At twin jets impingement, two wall jets are spreading radially each like a single jet impingement but reach and collide together at middle region between the two jets which called interaction zone. Jet interaction influence heat transfer in this region due to mix up of water streams and resulted higher turbulence. Depends on jets flow rate and nozzles distance, two flow regimes can be obtained due to interaction of water wall jets over stationary surface [7]. Distant nozzles and/or low flow rate jets produce thick calm film of water at interaction zone but closed nozzles and/or high flow rate jets induce thin fountain water with splashing.

Experimentation in mill condition is difficult and expensive to conduct and then, numerical modeling is a lower cost way of tuning final products properties in ROT cooling. However, the accurate thermal computation in ROT cooling is not easy to achieve. In fact, boiling is a complex, multiscale and fast transient phenomena and reliable boiling model which validated by high resolution thermal data is not available yet [8]. ROT studies mostly have noted heat transfer aspect but hydrodynamics of impingement flow due to long circular water jets in industrial scale received little attention despite important contribution in ROT cooling analysis. Among little researches on jet flow hydrodynamic in ROT application, Cho *et al.* [9] simulated a bank of water jet array impinging on a stationary target and found velocity and pressure profile along with flow depth. No heat transfer was considered.

Studying heat transfer and hydrodynamics of industrial long water jets impinging on cold and hot, moving and stationary test plates at a pilot-scale ROT facility is an ongoing project at University of British Columbia.

This work was supported by the Qatar National Research Foundation.

[1,3] *M.M.Seraj* (✉), *M,S. Gadala, Department of Mechanical Engineering, University of British Columbia* (seraj@mech.ubc.ca, gadala@mech.ubc.ca)

[2] *E. Mahdi, Department of Mechanical & Industrial Engineering, Qatar University, Doha, Qatar* (elsadigms@qu.edu.qa).

RECEIVED: 30, OCT., 2012; **REVISED:** 2, NOV., 2012; **ACCEPTED:** 14, NOV., 2012; **PUBLISHED:** 30, NOV., 2012.

010107029002992012000090

Experiments includes 19 *mm* pipe-type nozzles stand at variable heights (usually *H=1.5 m*) normal to horizontal test surface and discharging free surface circular long water jets at typical industrial flow rates (*Q* = 1.66-7.5e-4 *m3/s*). Most of researches on hydrodynamics of liquid jet have been done on short jets where unsteadiness and gravity are not noticeable. However, these long water jets are significantly sped up and contracted due to gravity at long distance between nozzle exit and test surface. Table 1 shows the jets parameters considering falling jet under gravitational acceleration. The impinging jets hit target surface at velocities many times larger than nozzle exit velocities and, in turn, impingement Re numbers are 50- 250% larger respect to the ones at nozzle outlet. Moreover, splattering and surface disturbances were usually occurred along the long water jets and transferred to the impingement flows. The experimental set up and procedure were reported before [3, 10]. In parallel, the numerical simulations of water jets have been performed [11] and also laminar and appropriate turbulent *k*-ε and *k*-ω models were used for the simulations of circular water jets in the experiments conditions. The simulations results for single and twin jets impinging on non-heated stationary flat surface and comparison with our experimental data and those from literature for short jets in impingement and parallel zones are presented in this paper. In the following, the numerical set up and simulations outcomes will be described.

TABLE 1
JETS PARAMETERS

d_n	$Q\times10$-4 (*m3/s*)	V_n (*m/s*)	d_{imp} (*mm*)	V_{imp} (*m/s*)	Re_n	Re_{imp}
19	2.5	0.88	7.6	5.49	16,690	41,666
	5	1.76	10.6	5.7	33,380	60,032
	7.5	2.65	12.6	6.03	50,068	75,627

2. NUMERICAL SIMULATION

Volume-of-fluid (VOF) [12] is a common multi-phase method for tracing interface of two immiscible fluids (e.g., water and air) in a mixture. VOF method is utilized in these simulations to obtain the free-surface of incoming jets before impingement and the free-surface of water film and wetting fronts and jets interaction after impingement. By defining a scalar parameter *f* for each phase (e.g., f_w for phase water), the volume fraction of the fluid inside every cell is determined and the phase is located in the domain; parameter *f* is zero for air (empty cell) and *f = 1* for water (filled cell) and is $0 < f < 1$ at interface. The continuity equation for volume-fraction of water, for example, can be used to track the air/water interface,

$$\frac{\partial}{\partial t}\left(f_w\rho_w\right) + \nabla.\left(f_w\rho_w\boldsymbol{U}\right) = 0 \tag{1}$$

The velocity vector $\boldsymbol{U}$ which is shared among phases will be found by solving one momentum equation for entire domain,

$$\frac{\partial}{\partial t}(\rho\boldsymbol{U}) + \nabla.(\rho\boldsymbol{U}\boldsymbol{U}) = -\nabla p + \nabla.[\mu(\nabla\boldsymbol{U} + \nabla\boldsymbol{U}^T)] + \rho\boldsymbol{g} \tag{2}$$

where *p* is pressure and $\boldsymbol{g}$ is gravity vector. Also, ρ and μ are density and viscosity, respectively, and are defined based on *f* of all phases.

The circular water jets were solved through transient flow Navier-Stokes equations using finite volume method along with VOF method by CFD program FLUENT. Laminar and two-equation *k-ε* and *k-ω* turbulent models were employed for jets numerical analysis. Turbulent *k-ε* model primarily was developed for high-Reynolds flows and is based on transport equations for turbulent kinetic energy *k* and turbulent dissipation rate *ε* [13] but turbulent *k-ω* model is mainly valid for low-Reynolds wall-bounded flow and is based on *k* and specific dissipation rate *ω* [14]. Turbulent *k-ε* model is very popular in simulation of industrial flow and heat transfer due to acceptable accuracy and reasonable computational cost. However, standard and traditional *k*-ε models are not recommended for impinging round jets where pressure gradient and strong streamline curvature and vortices are prominent [15]. Realizable *k-ε* model (RKE) [16] is an improved variant which successfully predicts the spreading rate of planar and round jets. Semi-empirical relations (wall functions) is utilized for viscosity-effected inner region (near wall) [13, 17] or it is resolved with one equation model of Wolfstein [18] and outer turbulent region is treated with turbulent *k*-ε model (two-layer model). RKE model was selected here because the boundary layer is not of particular interest in this work. On the other hand, turbulent *k-ω* model is appropriate for studying our thin water impingement layer which propagating radially over the target surface. The shear-stress transport *k-ω* model (SST) [19] allows for a gradual change from the near-wall layer to an outer turbulent flow of high-Reynolds number which was met in this study. It is a blend of standard *k-ω* model near the wall and a transformed *k-ε* model far from the wall. In the present study, laminar model and turbulent RKE and SST models were explored for single jet and RKE model for twin jet computations. The transient simulations were performed for long water jets at three flow rates of *Q* = 2.5, 5, 7.5e-4 *m3/s* (15, 30, 45 *L/min*) with high jet Reynolds numbers of 16,690- 50,100 according to the experiments conditions at our ROT facility (Table 1). The computations used first order discretization for time (available with VOF) and second order upwind schemes for momentum and turbulence model parameters which combined with a geo-reconstruction scheme for VOF discretization. The pressure and velocity were coupled by Pressure-Implicit with Splitting of Operators (PISO) scheme which recommended for transient simulations [15]. All computations were done with double precision accuracy. The normalized residuals were set at *O* (*10-4*) for continuity and at *O* (*10-6*) for velocity and turbulent parameters for solution convergence. The details of the above formulations and schemes are available in [15]. The air and water were considered at atmospheric condition with constant properties: for water ρ *= 998.2 kg/ m3* and μ *= 1.003e-3 kg/ m.s* and for air ρ *= 1.225 kg/ m3* and μ *= 1.7894e-5 kg/ m.s* and for water/air $\sigma = 0.0728\ N/m$. No thermal effect is considered here. The reported results are taken at long times after impingement when the impingement water layer fully covered target surface in the simulations and almost unchanged conditions were established. However, the twin jet simulation is undergoing and the available results are presented herein.

A. Domains, boundary conditions and meshes

Figure 1 shows 2D axisymmetric domain with jet axis for single jet computation. The free surface circular long water jet was modeled from nozzle exit down to target surface ($H = 1.5\ m$) where no-slip wall was considered ($u = v = 0$). The borders of the domain were pressure outlets where no water backflow was allowed (f = 0). At inlet, profile of velocity and turbulent quantities of nozzle exit were obtained by assuming a fully developed flow in nozzle pipe with 4% turbulence intensity. Figure 2 illustrates the 3D domain for twin jets computation where the main interest is jets interaction. It was sized by carefully observation of the multi-jets experiments in ROT facility [10] to include only inter-jets region as the first step of twin jets simulation. The domain is stepped down downstream of impingement zone and stepped up for jets interaction zone. Wall jets in parallel zone is very thin of *O (1e-1) mm* [10, 20] and in turn, 5 m above target surface was modeled, but in the middle 25 mm above surface modeled for jets interaction. The vertical symmetry planes were used to control the huge number of computational cells. The velocity profiles and turbulent parameters of incoming jets and surrounding air at inlets plans were derived from simulations of single jet at 50 mm above the target surface; this distance is about *7dimp* above the target surface for 2.5e-4 *m3/s* jets which was also used before in the simulation of jets impinging on moving surface [21]. All other boundaries are pressure outlets where open to outgoing flow but no water backflow is allowed. The target surface is no-slip stationary wall.

The two domains were meshed with non-uniform structural grids of rectangular cells which graded toward target surface and also, in impingement and interaction zones; see for example shaded areas 1, 2, 3 in Figure 1 where the jet traveling from inlet toward target surface and adjacent to wall surface where radial impingement flow was expanding over the surface. For twin jets simulation, the mesh was also clustered toward the symmetry plans in X- and Z-directions and in interaction zone between the jets where the wall jets meet and thick interaction film create. The mesh density varied according to laminar/turbulent models requirements and jet flow rates. The computations for mesh refinements were assessed at different flow rates, various models, and at before and after impingement until acceptable results were obtained. For example, the meshes were refined around the jet axis (regions 1 and 2) until the variations in impingement velocity and impingement time were less than 3 and 2 percent, respectively, for laminar simulation and less than 6 percent for all turbulent models. More details on comparisons of the meshes have been reported before [10, 20]. Therefore, the results in this paper are assumed to be grid independent. Also, the meshes had to maintain a continuous and uninterrupted developing of thin water sheet over the surface. Intermittencies were observed in cases of unsatisfactory meshes. Thus in addition to appropriate wall y^+, a discontinuous flow was avoided by adequate mesh refinement; $y^+ = \sqrt{\rho \tau_w} z / \mu$ where τw is the wall shear stress. Wall y^+ was kept smaller than 3 for SST simulations but it is $5 < y^+ < 10$ for RKE simulations using non-equilibrium wall functions. As such, smaller time step and more iteration were required and the simulations times were too long to get more accurate results. The grid for twin jet simulation has millions of cells and run on high performance multicore machine in parallel mode.

3. Results and Discussions

For incoming single jet before impingement, the computed axial velocities for all flow rates were compared with the experimental data and analytical solution of falling jet under gravity and good agreement was obtained particularly for RKE turbulent simulation. Average impingements velocities are almost equal the analytical ones. RKE and SST turbulent models had better performance than standard *k-ω* and k-ε versions at higher jet flow rate simulations. The axial velocity vectors around jet axis ($0 < r < dn/2$) are depicted in Figure 3for 5e-4 *m3/s*, for example, from RKE and SST turbulent single jet simulations.

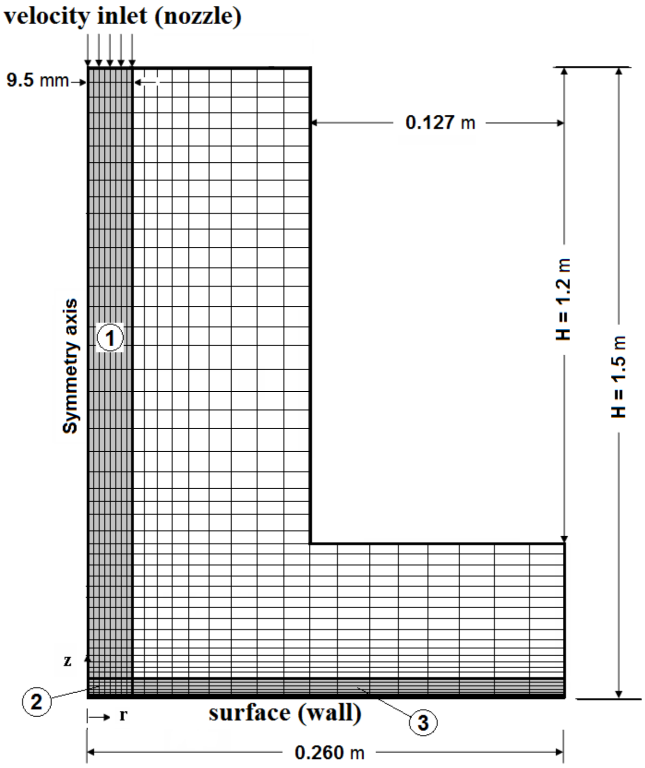

Fig. 1. Single jet simulation domain, and mesh (not scaled), other boundaries are pressure outlets.

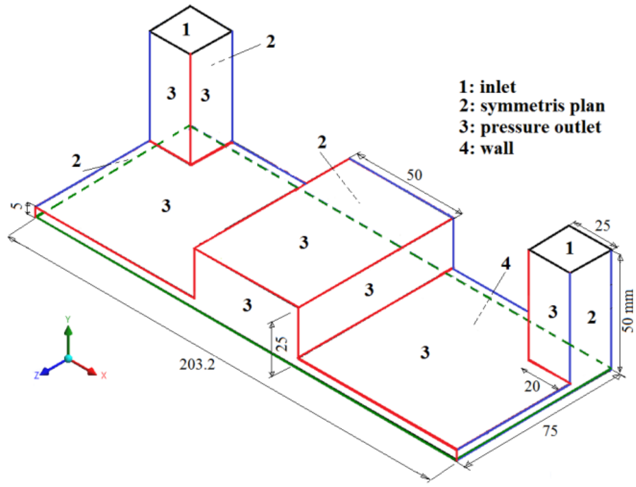

Fig. 2. Twin jets jet simulation: domain and boundary conditions

While the jets were going by flat velocity profile toward target surface, they were highly sped up and contracted due to significant effect of gravity (table 1) at both simulations. The jet velocity increased from 1.76 m/s at inlet to around 5.7 m/s at the surface. RKE and SST simulations gave close axial velocity for incoming jets. Although these velocity profiles were computed for uniform inlet velocity but effect of nozzle and inlet velocity is limited to vicinity of nozzle. Numerical investigations on different inlet velocity profiles (uniform, parabolic and 1/7th power) [22-23] demonstrate that velocity profile has noticeable influence until *H/dn <2* from nozzle and thereafter, similar velocity profiles are resulted near wall for larger nozzle elevation (*H/dn* > *2*). Moreover, other experimentations [24] reveals that nonuniformity inside turbulent liquid jet is diminished beyond (*3-5)d*. Therefore, the numerical velocity profiles from simulations of these industrial long jets (*H/dn* =79) and the resulted radial velocity and pressure of impingement water flow at surface in impingement and parallel zones are not sensitive to nozzle types and inlet velocity profiles.

Jet deceleration during impingement due to presence of target surface was also explored by these computations. It is exhibited previously for short water jets [25-26] that it starts at *z/d* = 0.5 above surface. Our simulations indicate that these long jets (*H/dn* = 79) decelerated before hitting the surface at *z/dimp* = 0.5 and beyond. The 2.5e-4 *m3/s* jet stopped speeding similar to short jet, but the 5e-4 *m3/s* jet axial velocity decreased *%5* at this level respects to impingement velocity and the 7.5e-4 *m3/s* jet velocity reduced *%10*. Higher jet Reynolds number, more pronounce wall effect on jet slowing at above *z/dimp* = 0.5 level. In turn, our numerical simulations predict that long water turbulent jets feel wall earlier than short jet but the jet speed reduction is not significant beyond *z/dimp* = 0.5. Surface disturbances of incoming jets were also studies. The jets surfaces between inlet and target surface before impingement were usually smooth although disturbances were initially detected similar to the experiments at ROT facility [27]. Actually, fluctuations in nozzle flow parameters were inevitable at ROT facility but uniform and unchanged profiles of inlet velocity and turbulence were implemented in these simulations. More experimental and numerical studies of long turbulent liquid jets (*H/dn>50*), relevant to industries, are required to investigating influence of flow features fluctuation at nozzle on jet surface disturbances, unsteadiness and splashing which are not seen in short liquid jets (*H/dn*< 5).

After impingement, the development of water flow adjacent to surface was traced by distribution of *f* contours. As an example, the propagation of wetting front and the free surface of the impingement water film are shown in Figure 4 during SST turbulent simulation of highest jet flow rate. The wetting front spread radially and moved gradually away from impingement point (*r* = 0). The thin water sheet formed with wavy free-surface and had round end (wetting front) due to surface tension. The front of liquid sheet finally exited computational domain and water film fully covered the surface. Very fine mesh was used in the simulation near the wall to keep the thin water sheet continuous. The computed flow expansion is comparable with the experimental observation [10].

The velocity of wetting front *Uf* can be found at any specified radius when the wetting front arrived there during the simulation. The frontal velocities *Uf* from the numerical simulations are compared with experimental data for all jet flow rates in Figure 5. The experiments were repeated many times because the jets were turbulent [10] and the bold curves are fittings to all experimental data collected for every jet flow rate. The frontal velocities steadily decrease with radius and agreement is good. Generally in the simulations, the impingement water films moved faster in the impingement zone, but it spread downstream slower than experiment. For *Ren* = 16,690 jet, the computed frontal velocity is larger up to approximately *r/dn< 6* where hydraulic jump was occurred and then becomes smaller than experimental ones. The wetting front *Uf* in *Ren* = 33,380 and 50,068 experiments are caught by the computed ones at around *r/dn* < *4* and *r/dn* ≈ *2*, respectively. The effect of impingement was noticeable on instant development of flow after impingement. Chaotic impingement and splashing were observed in the experiments while the jets impacted surface smoothly in the numerical simulations especially in SST simulations.

Impingement zone is extended up to where the effect of impingement vanished and further downstream is called parallel flow zone. Ochi et al [28] defined impingement zone as where the velocity and pressure is proportional to radius from stagnation point (*r* = *0*). He correlated linear variations for radial velocity *u* in impingement zone by experiments on short water jets impinging on unheated surface, similar to Liu's correlation [25]. The computed radial velocity profiles in impingement region are represented in figures 6 and 7 from turbulent simulations. Generally, the numerical velocities started increasing from zero at r = 0 linearly and then steadily grew near-linearly up to ~Vimp in agreement with the both proposed correlations [25, 28]. At very close to wall (very small z/dimp), the velocity is almost linear up to r/ dimp ~ 0.8 and, afterward, the velocity rise slowed down and flattens before reaching to a maximum value. At higher z/dimp, bigger peak of velocity is obtained which located at

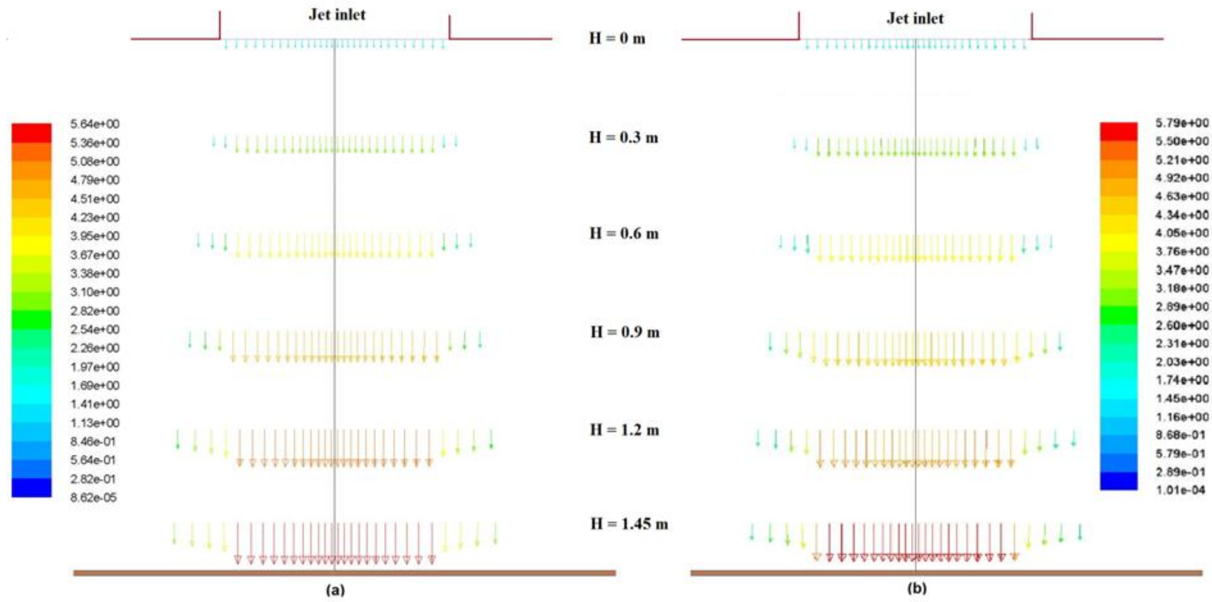

Fig.3. Axial velocity profiles of turbulent a long jet, Ren = 33,380, at different heights (a) RKE model (b) SST model

larger radius from stagnation point. For a given jet Re number and level z/dimp from wall, similar computed results are obtained among different flow rates computations during time processes. Gradient of velocity (B = du/dr) is also extracted from velocity computations because it is related to heat transfer in impingement zone; more heat is removed by impingement flow of higher velocity gradient [29].

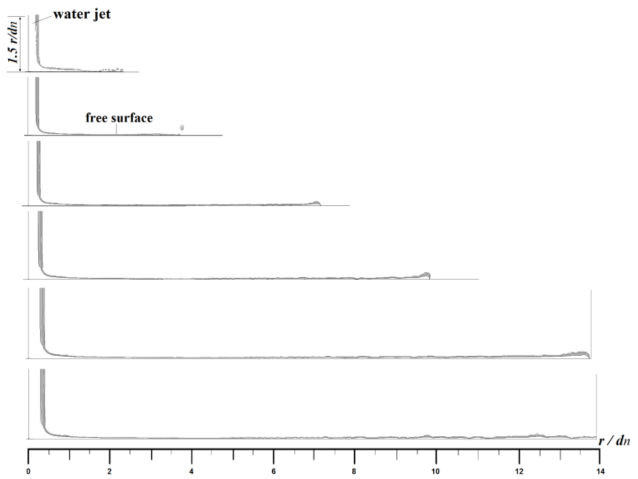

Fig. 4. Developing of thin impingement water film due to a long turbulent jet, Ren = 50,068, during SST simulation

Ochi measured B = 1.5625 [28] and Stevens found B ≈ 1.83 [29]. The velocity gradient of B ≈ 2 is found from the numerical velocity which is at least %10 larger than what is for short jets. Hence, higher cooling rates inside impingement zone would be expected from these long turbulent water jets. Again, this finding is not restricted to inlet velocity profile and nozzle type for long industrial water jets applications.

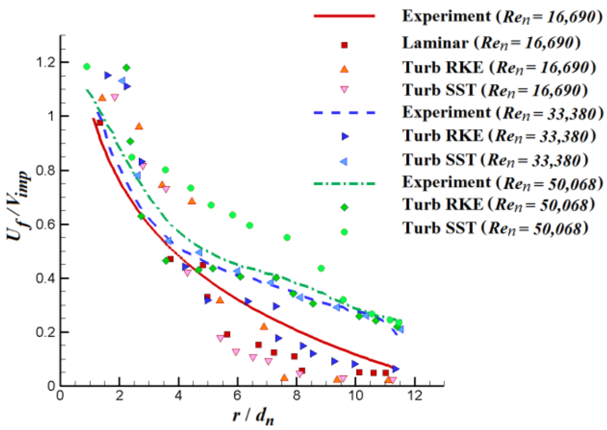

Fig.5. Experimental and numerical frontal velocities Uf for different jet flow rates

In ROT modeling, different boiling regime is assigned to different regions over hot surface, nucleate boiling regime to impingement region and transition/film boiling regimes to parallel region. The impingement region is demarcated from distribution of radial velocity and suggestion of r/dn = 1.28 by Ochi [28] for its dimension has been commonly accepted (see for example [30-31]). However, Steven and Webb [32] estimated impingement zone smaller as r/dn=0.75 for turbulent jet and Liu et al [33] confined this region to r/dn=0.787 for laminar jet from heat transfer data. Inspecting all computed velocities from our simulations of industrial long water jet shows that the velocity is linear or near-linear up to radius of (0.8-1)dimp at close to surface (z/dimp < 0.25) (see figures 7 and 8) and Ochi's prediction underestimates velocity in impingement zone and overpredicts the size of this region. Although impingement zone is much smaller than parallel zone but it is an influential region in heat transfer analysis of boiling jet impingement due to high rate of heat transfer detected there.

The highest coefficients of heat transfer and the largest surface temperature drop are occurred in this region during cooling. In an analysis of ROT cooling by round jets in mill conditions [30], for example, the extracted heat was found for impingement zone around %30 and for parallel zone over %50 of total heat removal in cooling of ROT stage.

Therefore, more care should be taken into account in using Ochi's estimation of impingement zone in ROT heat transfer modeling because heat flux in ROT cooling is in Mw/m^2 level and even small change in prediction of heat removal from hot metal plate is important. As such, accurate sizing of impingement zone is critical in ROT modeling due to significant portion of cooling taken in this small region. Although some studies were done in the past but experimentations and simulations of boiling flow hydrodynamics and associated heat transfer which focused on impingement zone and its extend in mill conditions is of great interest for industries. This numerical work is a step in this regard.

In parallel region, impingement water is flowing radially and losing momentum against wall drag as water sheet developing over the surface. The radial velocities of water flow at different vertical distances *z* from surface are presented in figure 8 for the lowest flow rate jet simulations. The velocity distribution is plotted up to free-surface where $0 < f < 1$. The velocity increased in impingement zone and then decreased in parallel zone. Negative velocity was observed at hydraulic jump place illustrated flow recirculation and demonstrated better by SST simulation. The jump was also observed in the experiments but no hydraulic jump in experiments and no negative velocity in simulations were detected at higher flow rates. As shown in figure 8, the water sheet was thin of $O(10e\text{-}1)$ *mm*.

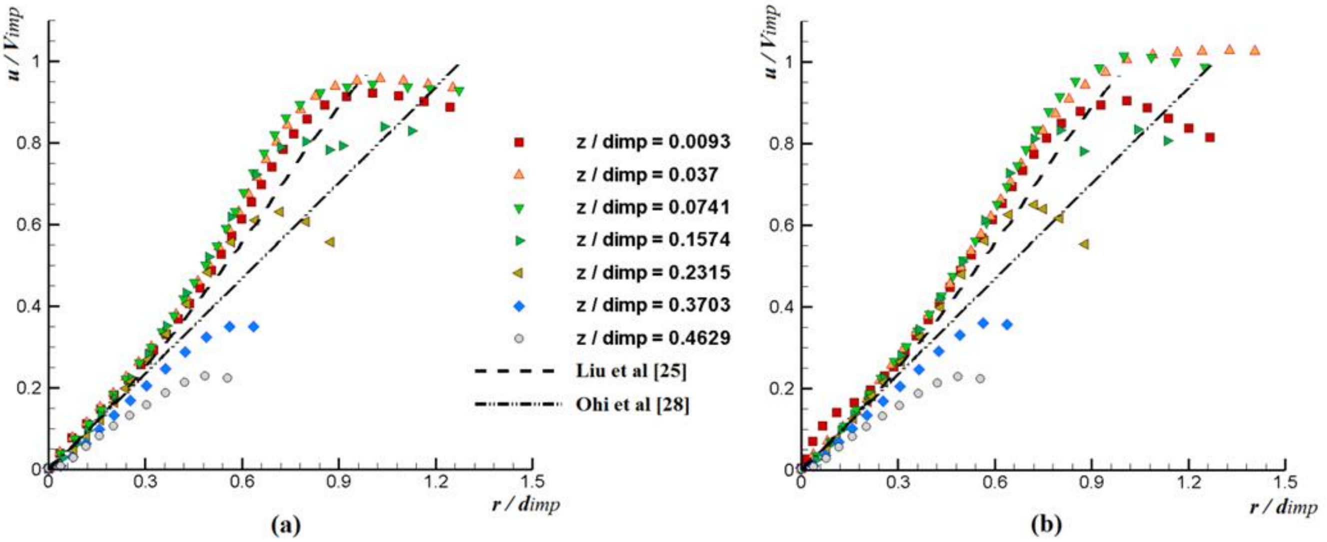

Fig.6. Radial velocity distributions in impingement zone at different levels, Ren = 33,380 long turbulent water jets simulations (a) RKE (b) SST

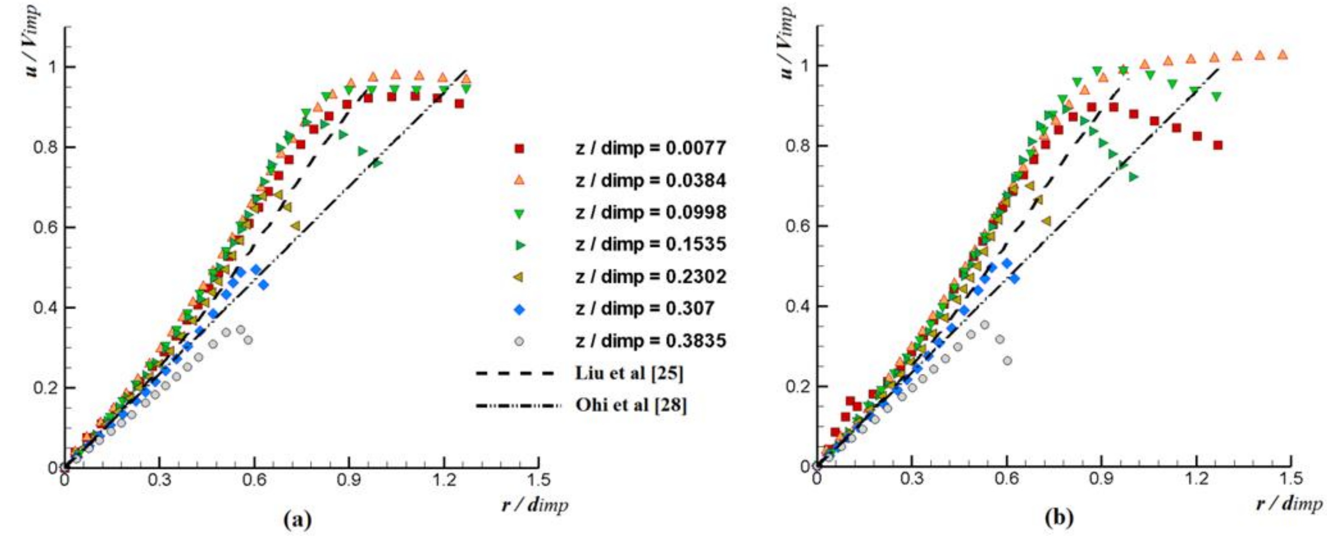

Fig.7. Radial velocity profiles in impingement zone at different levels, Ren = 50,068 long turbulent water jets simulations (a) RKE (b) SST

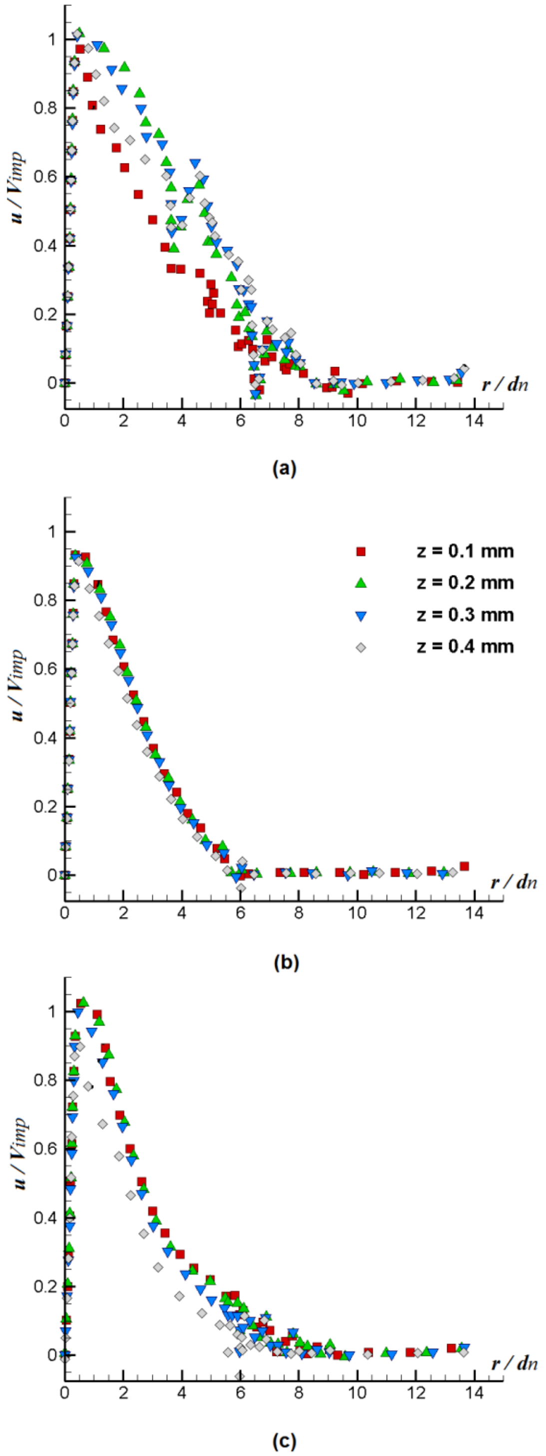

Fig.8. Radial flow velocities for Ren = 16,690 long jet over impingement surface in simulations, (a) Laminar (b) RKE (c) SST

For turbulent simulations, the free-surface stands almost at z = 0.4 *mm* while laminar fluid thickness was as low as z = *0.1 mm* in the middle of surface. Before the jump, laminar velocity variation was different from turbulent velocities in parallel zone because laminar water film is very thin with wavier free-surface and subject to intermittency but thicker turbulent films was formed over the surface. Due to jump occurrence, intermittency were also detected at upstream vicinity of hydraulic jump at turbulent simulations. Similar velocity profiles were drawn from higher *Re* long jets simulations. The thickness of water sheet increased according to jet *Re* and smooth propagation of water layer was obtained although, smoother and thicker layer usually resulted by SST turbulent simulation. At *Ren* = 50,068 jet simulation, RKE turbulent velocity profiles and film thickness are close to SST results which show that turbulent RKE model is also a choice for simulation of industrial high-Reynolds and wall-bounded flows.

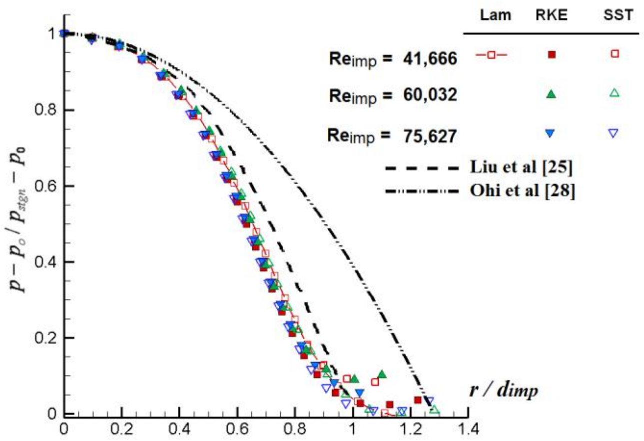

Fig.9. Pressure distributions along surface for long impinging water jets

For twin jets impingement on stationary surface, RKE turbulent numerical simulation has been started with lowest jet flow rate (Re_n = 16,690). Previous simulation of impingement flows on moving and nonmoving surfaces due to single long jet [20-21] demonstrate the performance of RKE turbulent model. The development of impingement flow was obtained from *f* contour and is shown on figure 10. The impingement water films from each jet was expanding radially over target surface similar to single jet impingement and then was colliding together and interacting at the middle between the two jets (figure 10a). Thereafter, the radial wall jets gradually covered impingement surface and the jets interaction was growing progressively. The wetting front propagation of each wall jet and collision at interjet symmetry plane illustrates better evolution of interaction of twin liquid jets during time (figure 10b). The round wetting fronts met and joined together and created thick water film which was widening between the two jets. The dome-shape interaction film was calm and no splashing was observed. The experiments of twin water jets in ROT [10] represent same type of jets interaction with good timing for expanding over surface and start of interaction.

The twin jets interaction is plotted by *f* contours at different plane levels parallel to impingement surface in figure 11 at t = 0.9 sec. As shown, the water layer of 0.1 mm is fully covered the surface (z = 0 mm) at this time and the thick water film as high as 8 cm is accumulated in interaction zone. The water film thickness is increasing toward jet-to-jet axis along the line where the two radial streams meet directly because of higher velocity of wall jets toward jet-to-jet axis. Examining turbulent parameters

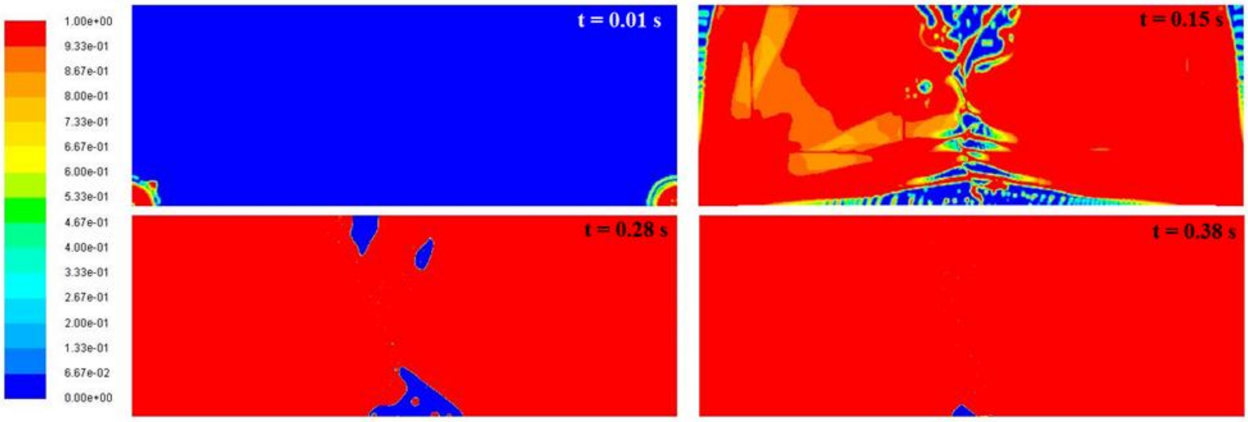

(a)

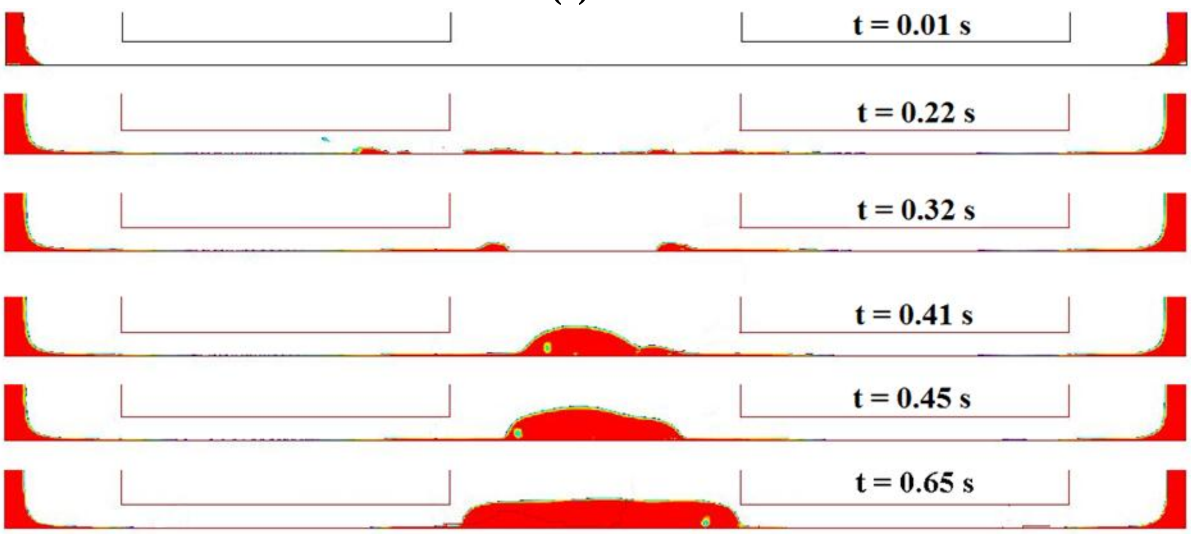

(b)

Fig 10. Development of impingement flow and interaction due to twin jets (Ren = 16,690) (a) over target surface (b) wetting front at interjet-symmetry plan, red color shows water (f = 1)

showed low level of turbulent kinetic energy and turbulent intensity at interaction zone compare with inlet and impingement zone and then calm interaction according to the experiment at ROT facility [10] is reproducing. These simulations are ongoing with optimizing cell numbers and minimizing computational time to replicate the multiple liquid jets interactions with industrial scale parameters.

4. CONCLUSION

The hydrodynamics of long circular single and twin free-surface water jets with typical industrial height and jet flow rates (Re_n = 16,690 - 50,068) impinging normally on flat horizontal surface was studied numerically by laminar and turbulent RKE k-ε and SST k-ω models. The computed velocity profiles of incoming jets at long distance between nozzle outlet and target surface were shown great acceleration of these long jets (Re_{imp} = 41,666 - 75,627) due to major effect of gravity. The long water jets stopped speeding before impingement similar to short jets. However, the higher Re long jets started reduction at further distance above wall although the speed reduction is not significant up to z/d_{imp} = 0.5 where the short jet deceleration began.

The impingement water flow over surface due to long jets present some common features with short jet. The spreading of thin water layers over impingement surface were drawn and found in good agreement with the experimental data at same conditions from ROT facility. SST turbulent model obtained smoother development of impingement radial flow during simulations and then RKE k-ε turbulent model. In impingement zone, velocity increases linearly/ near-linearly up to r/d_{imp} = 0.8 similar to predicted velocity distribution for short jets if jet velocity and jet diameter adjusted by impingement velocity and diameter, respectively, in the related correlations. However, velocity gradient for these long turbulent jets is found about 10% higher than short jet which indicates better performance of long liquid jets in heat extraction in impingement zone than short liquid jets. In addition, the computed velocities suggest smaller size of impingement zone respect to the one used commonly in ROT modeling which have an impact on prediction of heat removal in ROT cooling. Also, computed local pressure due to impinging long jets was beyond 80% of ambient pressure at $r/d_{imp}<0.5$ and thus, the influence of pressure on water saturation temperature is prominent in this region. The

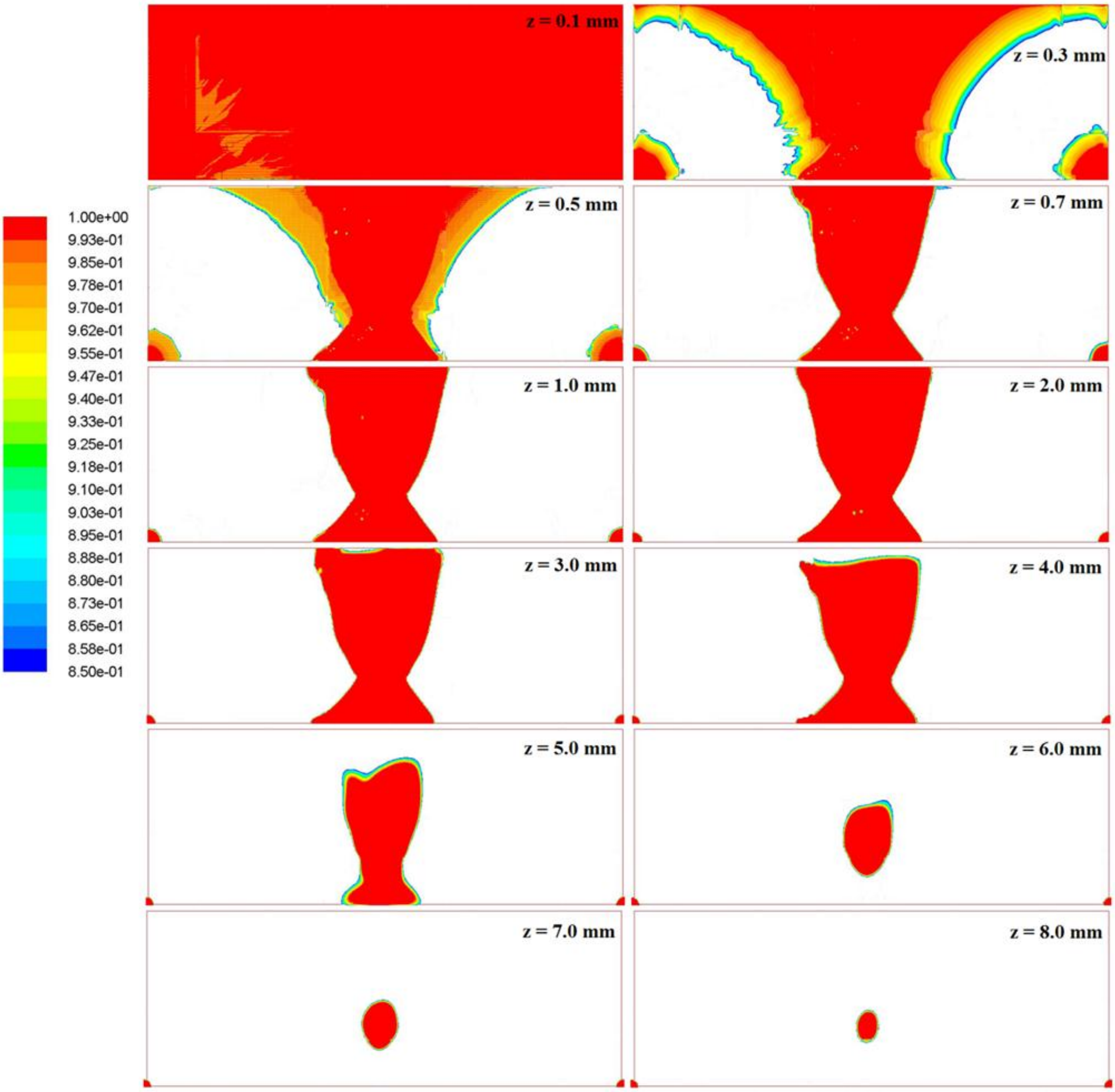

Fig. 11. Impingement flow development and interaction due to twin jets (Ren = 16,690), red color shows water (f = 1)

effect of corrected saturation temperature against local pressure at the boiling heat transfer correlations was assessed up to 9% in estimation of heat flux which is essential in ROT cooling where the heat fluxes are very high (up to 10 Mw/m^2).

The outcomes of these hydrodynamics simulations demonstrate the necessity for more experimentations and computations on long turbulent water jet instead of relying solely on short jet studies in ROT modeling efforts in mill condition. First, the impingement zone should be delineated accurately beneath each jet over hot surface. Second, variability of saturation temperature of water in impingement zone as a high pressure gradient region should be taken into calculation of heat transfer analysis at ROT stage.

The twin jets simulation represents interaction of two radial wall jets and occurrence of nonsplashing interaction type where thick water layer formed in interaction zone accordance to the experimentations of multiple long water jets in ROT facility. The water layer thickness is increased toward jet-to-jet axis. The effect of jet flow rate on jet kind of jets interaction is to be studied soon.

ACKNOWLEDGMENT

This research was supported by a grant fund NPRP 09 - 507 - 2 – 191 from the Qatar National Research Foundation (QNRF), Qatar.

REFERENCES

[1] M. K. Sung and I. Mudawar, "Single-phase and two-phase heat transfer characteristics of low temperature hybrid micro-channel/micro-jet impingement cooling module," *International Journal of Heat and Mass Transfer,* vol. 51, pp. 3882-3895, 2008.

[2] R. Viskanta and F. Incropera, "Quenching with liquid jet impingement," in *Heat and Mass Transfer in Materials Processing*, I. Tanasawa and N. Lior, Eds., ed: Hemisphere Publishing New York, 1990, pp. 455-476.

[3] G. Franco, M. Wells, and M. Militzer, "Effect of Nozzle Configuration on Cooling of a Hot Moving Steel Plate," *Canadian Metallurgical Quarterly,* vol. 48, pp. 197-205, 2009.

[4] D. Wolf, F. Incropera, and R. Viskanta, "Jet impingement boiling," *Advances in heat transfer,* vol. 23, pp. 1-132, 1993.

[5] J. Stevens, Y. Pan, and B. Webb, "Effect of nozzle configuration on transport in the stagnation zone of axisymmetric, impinging free-surface liquid jets: Part 1-turbulent flow structure," *Journal of Heat Transfer* vol. 114, 1992.

[6] J. Hammad, Y. Mitsutake, and M. Monde, "Movement of maximum heat flux and wetting front during quenching of hot cylindrical block," *International journal of thermal sciences,* vol. 43, pp. 743-752, 2004.

[7] R. Kate, P. Das, and S. Chakraborty, "An experimental investigation on the interaction of hydraulic jumps formed by two normal impinging circular liquid jets," *Journal of Fluid Mechanics*, vol. 590, pp. 355-380, 2007.

[8] G. Son and V. K. Dhir, "Numerical simulation of nucleate boiling on a horizontal surface at high heat fluxes," *International Journal of Heat and Mass Transfer,* vol. 51, pp. 2566-2582, 2008.

[9] M. J. Cho, B. G. Thomas, and P. J. Lee, "Three-Dimensional Numerical Study of Impinging Water Jets in Runout Table Cooling Processes," *Metallurgical and Materials Transactions B,* vol. 39, pp. 593-602, 2008.

[10] M. M. Seraj, S. A. Ghani, and M. S. Gadala, "Hydrodynamics of Single and Twin Long Free Circular Water Jets in Industrial Scale," in *World Academy of Science, Engineering and Technology*, Switserland, pp. 332-339, 2012.

[11] F. Xu and M. S. Gadala, "Heat transfer behavior in the impingement zone under circular water jet," *International Journal of Heat and Mass Transfer,* vol. 49, pp. 3785-3799, 2006.

[12] C. W. Hirt and B. D. Nichols, "Volume of fluid (VOF) method for the dynamics of free boundaries," *Journal of computational physics,* vol. 39, pp. 201-225, 1981.

[13] B. E. Launder and D. Spalding, "The numerical computation of turbulent flows," *Computer methods in applied mechanics and engineering,* vol. 3, pp. 269-289, 1974.

[14] D. C. Wilcox, *Turbulence modeling for CFD* vol. 2: DCW industries La Canada^ eCalifornia California, 1998.

[15] A. Fluent, "Ansys Fluent 13.0 user guide," *ANSYS Inc*, 2010.

[16] T. H. Shih, W. W. Liou, A. Shabbir, Z. Yang, and J. Zhu, "A new k-ϵ eddy viscosity model for high reynolds number turbulent flows," *Computers & Fluids,* vol. 24, pp. 227-238, 1995.

[17] S. E. Kim and D. Choudhury, "A near-wall treatment using wall functions sensitized to pressure gradient," *Separated and complex flows- 1995,* pp. 273-280, 1995.

[18] M. Wolfshtein, "The velocity and temperature distribution in one-dimensional flow with turbulence augmentation and pressure gradient," *International Journal of Heat and Mass Transfer,* vol. 12, pp. 301-318, 1969.

[19] F. Menter, M. Kuntz, and R. Langtry, "Ten years of industrial experience with the SST turbulence model," in *Turbulence, heat and mass transfer*. vol. 4, K. Hanjalic, Y. Nagano, and M. Tummers, Eds., ed: Begell House Inc., 2003, pp. 625-632.

[20] M. Seraj and M. Gadala, "Numerical Investigation of an Impingement Flow due to a Free Surface Axisymmetric Long Water Jet," *AMSE IMECE2011*, USA, pp. 343-354, 2011.

[21] M. M. Seraj and M. S. Gadala, "NonCircular Hydraulic Jump on a Moving Surface due to an Impinging Circular Free Surface Jet of Water," *steel research international,* vol. 83, pp. 653-670, 2012.

[22] H. Fujimoto and S. Dejima, "Numerical Analysis and Heat transfer of a Free Surface Circular Jet Impinging onto a Substrate," A*SME IMECE2007*, Seattle, USA, pp. 1117-1124, 2007.

[23] A. Y. Tong, "A numerical study on the hydrodynamics and heat transfer of a circular liquid jet impinging onto a substrate," *Numerical Heat Transfer: Part A: Applications,* vol. 44, pp. 1-19, 2003.

[24] J. Lienhard, "Liquid jet impingement," *Annual Review of Heat Transfer,* vol. 6, pp. 199-270, 1995.

[25] Liu X., L. A. Gabour, and J. H. Lienhard V, "Stagnation-point heat transfer during impingement of laminar liquid jets: analysis including surface tension," *Journal of heat transfer,* vol. 115, pp. 99-105, 1993.

[26] Stevens J and W. B. W, "Measurements of flow structure in the stagnation zone of impinging free-surface liquid jets," *International Journal of Heat and Mass Transfer* vol. 36, pp. 4283-4286, 1993.

[27] M. M. Seraj, "Hydrodynamics of circular free-surface long water jets in industrial metal cooling," PhD, Mechanical Engineering, University of British Columbia, Canada, 2011.

[28] T. Ochi, S. Nakanishi, and S. ISHIGAI, "Cooling of a hot plate with an impinging circular water jet," in *Multiple Flow and Heat Transfer III, Part A: Fundamentals*, 1983, pp. 428-429.

[29] Y. Pan, J. Stevens, and B. Webb, "Effect of nozzle configuration on transport in the stagnation zone of axisymmetric, impinging free-surface liquid jets: Part 2-local heat transfer," *Journal of Heat Transfer,* , vol. 114, pp. 880-886, 1992.

[30] J. Filipovic, R. Viskanta, F. P. Incropera, and T. A. Veslocki, "Cooling of a moving steel strip by an array of round jets," *Steel research,* vol. 65, pp. 541-547, 1994.

[31] A. Koldin and N. Platonov, "A study of heat transfer in the surface layer of metal during the impingement of a liquid jet," *Thermal Engineering,* vol. 55, pp. 223-227, 2008.

[32] J. Stevens and B. Webb, "Local heat transfer coefficients under an axisymmetric, single-phase liquid jet," *Journal of Heat Transfer* vol. 113, pp. 71-78, 1991.

[33] X. Liu, J. Lienhard, and J. Lombara, "Convectiwe heat transfer by impingement of circular liquid," *Journal of heat transfer,* vol. 113, pp. 571-582, 1991.

Available online at:
http://tsest.org/index.php/TCMS/article/view/90

Download full text article at:
http://tsest.org/index.php/TCMS/article/download/90/50

Cite this work as:
M. M. Seraj, E. Mahdi, and M. S. Gadala, "Numerical Assessments of Impingement Flow over Flat Surface due to Single and Twin Circular Long Water Jets" *TSEST Transaction on Control and Mechanical Systems*, Vol. 1, No. 7, PP. 290-299, Nov., 2012.